

The Reconfigurable Omnidirectional Articulated Mobile Robot (ROAMeR)

Qiushi Fu, Xiaobo Zhou and Venkat Krovi*

Abstract Articulated Wheeled Robot (AWR) locomotion systems consist of a chassis connected to sets of wheels through articulated linkages. Such articulated "leg-wheel systems" facilitate reconfigurability that has significant applications in many arenas, but also engender constraints that make the design, analysis and control difficult. In this paper we study this class of systems in the context of design, analysis and control of a novel planar reconfigurable omnidirectional wheeled mobile robot. This AWR distinguishes itself from existing wheeled mobile robots by having the capability to change the location of its wheels relative to the chassis. We first extend a twist-based modeling approach to systematically construct the symbolic kinematic model for a general class of AWR before specializing it to our planar AWR example. We then develop a kinematic redundancy resolution scheme to coordinate the motion of the articulated legs and wheels. Two generations of physical prototypes were developed, refined and tested using simulation/virtual prototyping and real-time/hardware in the loop methodologies. Representative results from both sets of approaches are presented to illustrate combined locomotion and reconfiguration.

1 Motivation

The Reconfigurable Omnidirectional Articulated Mobile Robot (ROAMeR) is a highly maneuverable Articulated Wheeled Robot (AWR) capable of moving omnidirectionally in the plane while possessing the ability to change its internal configuration. The characteristic feature of such AWR systems is the attachment of the multiple wheels to a common chassis via articulated chains, which facilitates (active or passive) repositioning of the wheel with respect to chassis during locomotion. Such leg-wheeled systems have many advantages over both traditional wheeled

Qiushi Fu, Xiaobo Zhou and Venkat Krovi*
Mechanical and Aerospace Engineering, SUNY at Buffalo, Buffalo, New York, 14260 e-mail: vkrovi@eng.buffalo.edu

systems and legged systems in various applications as planetary exploration [8], forestry [4], rescue operations and wheelchairs [11].

However, articulated-wheeled-robotic systems are highly constrained mechanical systems subjected to both holonomic constraints (due to the multiple closed-loops) and nonholonomic constraints (due to disc-wheel/ground contacts). Violation of these constraints (e.g. typically in terms of slipping and skidding at the ground-wheel contacts), causes both energy-wastage and estimation-uncertainty. Considerable research has focused on both enhanced kinematic-design, such as suspension mechanisms [8] to avoid constraint violation without sacrificing payload capacity or increasing power consumption, and active-coordinated-control for enhancing mobility, stability and/or traction [12, 9].

Kinematic modeling of ordinary wheeled robots (OWRs, which can be seen as a subset of AWRs) has been dealt with extensively. Muir and Newman [5] derived the equation of motion of OWRs using matrix transformation. Campion et al. [1] classified OWRs based on kinematic models developed using vector approach and nonholonomic constraints. Yi and Kim [13] presented modeling of omnidirectional wheeled robots with slipping. Less attention has been focused on AWRs. Grand et al. [3] presented a general geometric modeling approach and controlled the locomotion and posture separately. Tarokh and McDermott [10] used symbolic derivatives of transformation matrices with consideration of wheel slip and discussed three different kinematic forms for passive rovers. Choi and Sreenivasan [2] constructed the kinematic model using screws and proposed a force distribution algorithm.

We focus on developing a systematic and general-purpose modeling, analysis and operational framework, suitable for both the design and control of such Articulated Wheeled Robotic Systems. To the best of our knowledge, twist- and wrench-based approaches have not been used to analyze articulated-systems with rolling wheel-ground contacts, despite previously being used to analyze motion and force capabilities of in-parallel articulated-mechanical-systems (such as parallel manipulators or multifinger grasping). Thus, the contribution of this paper lies in extending the twist- and wrench-based modeling framework to such Articulated Wheeled Robotic Systems (and subsuming the extant specialized approaches for ordinary wheeled robots [1]), and automating this process by use of symbolic analysis methods to facilitate the rapid analysis of various AWR designs. Finally, we illustrate this process in the context of design, analysis and experimental validation of an omnidirectional planar articulated-wheeled robot called the ROAMeR.

2 Technical Approach

The ROAMeR has a main chassis/body connected to three in-parallel articulated-legs by actuated-revolute joints (hip). Each articulated-leg is then connected to an offset-caster wheel which is actively-steered (knee) and actuated. The relative position of the wheels with respect to the chassis can be changed by varying the angle of the posture joints that connect the links and chassis (hip and knee).

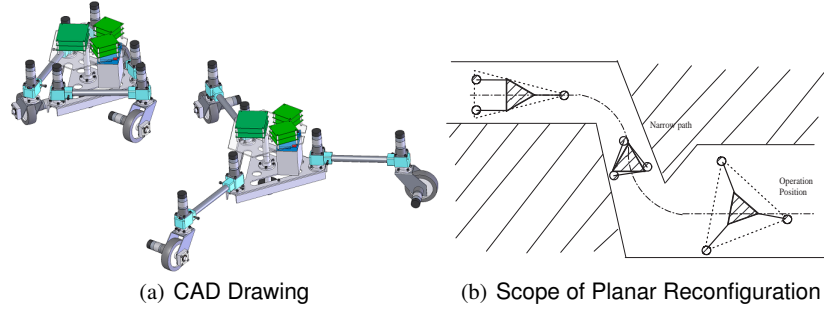


Fig. 1 The Planar Reconfigurable Omnidirectional Articulated Mobile Robot (ROAMeR) Design

2.1 Twist Based Formulation

A general model of AWR is shown in Fig.2, we define an inertial frame of reference $\{F\} = (O_f, \mathbf{X}, \mathbf{Y}, \mathbf{Z})$, and at any time, the robot has an instantaneous frame $\{B\} = (O_b, \mathbf{b}_x, \mathbf{b}_y, \mathbf{b}_z)$ attached to its body that moves with the robot, where O_b is the point of interest on the robot (it is often convenient to choose center of mass, geometric center of the chassis, or the equipment mounting position as the point of interest). The configuration of the main chassis could be defined as $[x \ y \ z \ \phi \ \theta \ \psi]^T$ with respect to the inertial frame.

In the most general case, the chassis is supported by n serial branches with each chain possessing m joints and ending in a wheel. Each wheel has a coordinate frame $\{W\} = (O_w, \mathbf{w}_x, \mathbf{w}_y, \mathbf{w}_z)$ attached to the wheel axle (for simplicity, we omit the subscript i indexing each branch), O_w is the center of the wheel and \mathbf{w}_z lies on the wheel axle. The dashed line in the figure between the chassis and the wheel represents the articulated linkage between these two frames, including the steering and suspension mechanism. We define ${}^B A_0$ the transformation between body frame and joint 1 frame, ${}^{j-1} A_j, j = 1, 2, \dots, m-1$ the transformation between joint j and joint $j+1$ frame, ${}^{m-1} A_m$ the transformation between joint m frame and wheel frame, which simplifies determination of homogeneous transformation matrices as well as the determination of twist vectors in their immediately preceding frames. These transformations can be expressed easily using D-H parameters.

Each wheel is assumed to be represented by a rigid disc with a single point of contact with the terrain surface. The wheel plane is defined at the center of the wheel and perpendicular to the wheel axle \mathbf{w}_z , that is, the plane formed by \mathbf{w}_x and \mathbf{w}_y . A contact plane is defined perpendicular to the wheel plane at the contact point. The multi-point contact case offers greater challenges, both for modeling as well as for sensing/estimating the contact locations and is beyond the current scope. For the single point contact, a contact frame, $\{C\} = (O_c, \mathbf{c}_x, \mathbf{c}_y, \mathbf{c}_z)$ is defined as the contact frame assigned at each wheel's contact point as illustrated in the figure, where \mathbf{c}_z is a unit vector in the wheel plane and normal to the contact plane at the point of contact,

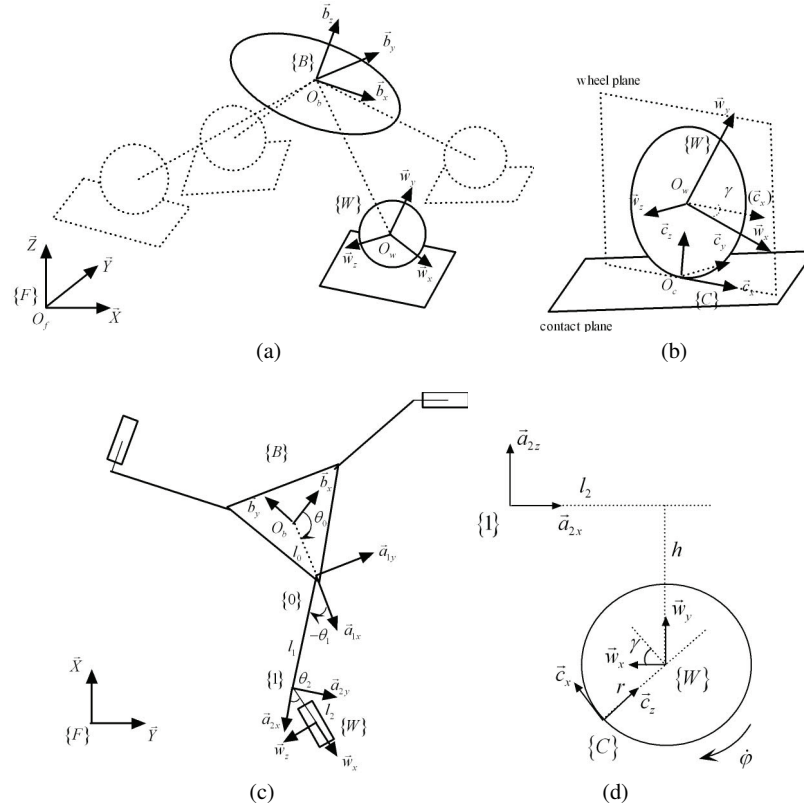


Fig. 2 (a) A General Model of AWR; (b) Model of Wheel Ground Contact; (c) Body Frames of ROAMeR; (d) Wheel-Leg Frame

that is, a vector pointing to the center of the wheel. $\mathbf{c}_x = \mathbf{c}_z \times \mathbf{w}_z$, and $\mathbf{c}_y = \mathbf{c}_z \times \mathbf{c}_x$. γ is the contact angle defined as the angle between \mathbf{c}_x and \mathbf{w}_x , since \mathbf{c}_x always lies in the wheel plane. This angle can be measured using force sensor on the wheel axle or be estimated. It is one of the most important factors for AWRs moving on uneven terrain. For AWRs moving on flat surface, this angle is usually constant and less important. The transformation between the wheel frame and contact frame is denoted by the homogeneous transformation

$$w_{AC} = \begin{bmatrix} \cos \gamma & 0 & -\sin \gamma & r \sin \gamma \\ \sin \gamma & 0 & \cos \gamma & -r \cos \gamma \\ 0 & -1 & 0 & 0 \\ 0 & 0 & 0 & 1 \end{bmatrix}. \quad (1)$$

The overall transformation from body frame to one contact frame can be found as

$${}^B A_C = {}^B A_W {}^W A_C = {}^B A_0 {}^0 A_1 \cdots {}^{m-1} A_W {}^W A_C. \quad (2)$$

We follow the notation of [6] broadly, and take advantage of symmetric design for a staged derivation - first for the in-parallel articulated branches with the subsequent assembly into a system model. The contact twist expressed in contact frame as:

$${}^C [{}^F V_C] = [{}^C A d_B]^B [{}^F V_B] + B \dot{q} \quad (3)$$

where $B = [{}^C [{}^{A1} t_{A2}] \cdots {}^C [{}^{Am-1} t_{Am}] {}^C [{}^{Am} t_W] {}^C [{}^W t_C]]$ is an assembled-twist matrix and $\dot{q} = [\dot{\theta}_1 \cdots \dot{\theta}_{m-1} \dot{\theta}_m \dot{\phi}]^T$ is a vector consists of m joint variables in the chain and the wheel rotational velocity $\dot{\phi}$. The pure rolling contact condition at the contact point can be represented as

$$S^T {}^C [{}^F V_C] = [0 \ 0 \ 0]^T \quad (4)$$

where $S^T = [I_{3 \times 3} \ 0_{3 \times 3}]$ is a wrench basis matrix that represents the direction where force can be exerted (which selects the first three rows of the twist vector and restricts the translational motion at the contact point). For one branch of an AWR, if pure rolling condition is assumed, we can rewrite the Eq. 4 as:

$$-S^T [{}^C A d_B]^B [{}^F V_B] = S^T B \dot{q}. \quad (5)$$

Concatenating the equations for all branches we can obtain the system-level kinematic equations as:

$$M^B [{}^F V_B] = J \dot{q}. \quad (6)$$

The D-H parameters for the ROAMeR system are shown in Table 1.

Table 1 D-H Parameters of the ROAMeR

| Joint | α | a | d | θ |
|----------------------|----------|-------|------|------------|
| 1 posture $\{A_0\}$ | 0 | l_0 | 0 | θ_0 |
| 2 steering $\{A_1\}$ | 0 | l_1 | 0 | θ_1 |
| 3 driving $\{W\}$ | $\pi/2$ | l_2 | $-h$ | θ_2 |

Specializing to the planar case and noting that $\dot{X}_b = [\dot{x}_b \ \dot{y}_b \ \dot{\psi}_b]^T$ and $\dot{q}_A = [\dot{\phi}_1 \ \dot{\theta}_{12} \ \dot{\theta}_{11} \ \dot{\phi}_2 \ \dot{\theta}_{22} \ \dot{\theta}_{21} \ \dot{\phi}_3 \ \dot{\theta}_{32} \ \dot{\theta}_{31}]^T$ we can then assemble the overall kinematic equation from all three branches as:

$$P_A \dot{X}_b = Q_A \dot{q}_A \quad (7)$$

where

$$P_A = \begin{bmatrix} c_{012}^1 & s_{012}^1 & l_0 s_{12}^1 + l_1 s_2^1 \\ -s_{012}^1 & c_{012}^1 & l_0 c_{12}^1 + l_1 c_2^1 + l_2 \\ c_{012}^2 & s_{012}^2 & l_0 s_{12}^2 + l_1 s_2^2 \\ -s_{012}^2 & c_{012}^2 & l_0 c_{12}^2 + l_1 c_2^2 + l_2 \\ c_{012}^3 & s_{012}^3 & l_0 s_{12}^3 + l_1 s_2^3 \\ -s_{012}^3 & c_{012}^3 & l_0 c_{12}^3 + l_1 c_2^3 + l_2 \end{bmatrix}$$

$$Q_A = - \begin{bmatrix} r & 0 & l_1 s_2^1 & 0 & 0 & 0 & 0 & 0 \\ 0 & l_2 & l_1 c_2^1 + l_2 & 0 & 0 & 0 & 0 & 0 \\ 0 & 0 & 0 & r & 0 & l_1 s_2^2 & 0 & 0 \\ 0 & 0 & 0 & 0 & l_2 & l_1 c_2^2 + l_2 & 0 & 0 \\ 0 & 0 & 0 & 0 & 0 & 0 & r & 0 \\ 0 & 0 & 0 & 0 & 0 & 0 & 0 & l_1 s_2^3 \\ 0 & 0 & 0 & 0 & 0 & 0 & 0 & l_2 \end{bmatrix}.$$

2.1.1 Kinematic Control

We examine issues related to the control of locomotion and reconfiguration within this system with significant kinematic redundancy. The ROAMeR has 9 active degrees-of-freedom available to control a 3-dimensional locomotion task, encoded as a Cartesian trajectory tracking task for the chassis center-of-mass frame of reference $X_b = [x_b \ y_b \ \psi_b]^T$. Effective control of the highly articulated system requires various degrees-of-freedom to be carefully coordinated, while remaining consistent with 6 kinematic constraints. On the other hand, such redundancy can be exploited to secondarily achieve system reconfiguration, encoded as a position regulation task for a subset of joint variables $\eta = [\theta_{11} \ \theta_{21} \ \theta_{31}]^T$ by way of a null-space controller [7]. Since Q_A is always full rank and has more columns than rows, an expression for the resolved joint-rates may be written as:

$$\dot{q}_A = Q_A^\# P_A \left(\dot{X}_b^d + K_X (X_b^d - X_b) \right) + [I - Q_A^\# Q_A] Z \quad (8)$$

where $Q_A^\# = Q_A^T (Q_A Q_A^T)^{-1}$ is the Moore-Penrose generalized inverse of Q_A , and $Z = -\nabla V$ is a potential function that drives the posture error to zero, where $V = K_\theta \left[(\theta_{11} - \theta_{11}^d)^2 + (\theta_{21} - \theta_{21}^d)^2 + (\theta_{31} - \theta_{31}^d)^2 \right]$. The particular solution part of Eq. 8 controls the robot to achieve the primary Cartesian trajectory-following task (with closed-loop correction) while the homogeneous solution designed to achieve the secondary task, leg position regulation. We use 9 independent PID controllers to control each joint within an xPC Target based Hardware-in-the-Loop (HIL) control framework. The control diagram is shown in Fig. 3.

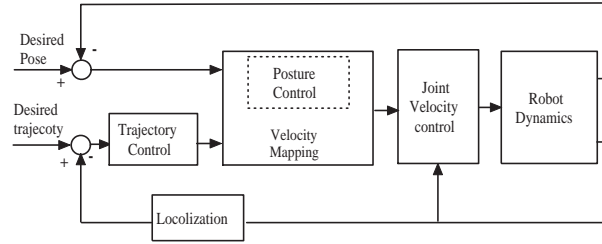


Fig. 3 Kinematic Control Scheme

3 Experiments

3.1 Hardware-In-the-Loop Prototyping

Two generations of physical prototypes were built and tested, as shown in Fig. 4. The first prototype was built with RC-servo joint actuation coordinated by Lynxmotion servo controller board receiving velocity setpoint commands serially from a MATLAB-based open-loop controller. It allowed us to verify initial real-world feasibility of the simultaneous trajectory-following and reconfiguration approach.

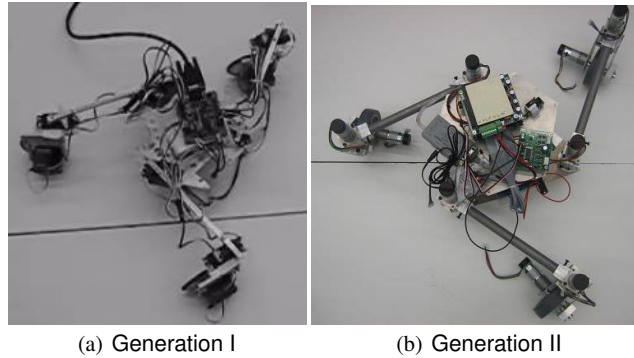


Fig. 4 Physical Prototypes

All further testing was conducted with a more rugged second-prototype that was constructed with machined structural components, battery-operation, reliable actuation and sensing (DC motors/encoders) controlled by an onboard PC104 platform running an xPC Target HIL controller. We use a real-time (100Hz) motion-tracking system (OptiTrack) Operating with the XPC target environment to provide ground truth measurement of the performance of the system. We note that this system could

optionally provide real-time global sensing which can be fused with odometry to improve performance, however this aspect is not reported here.

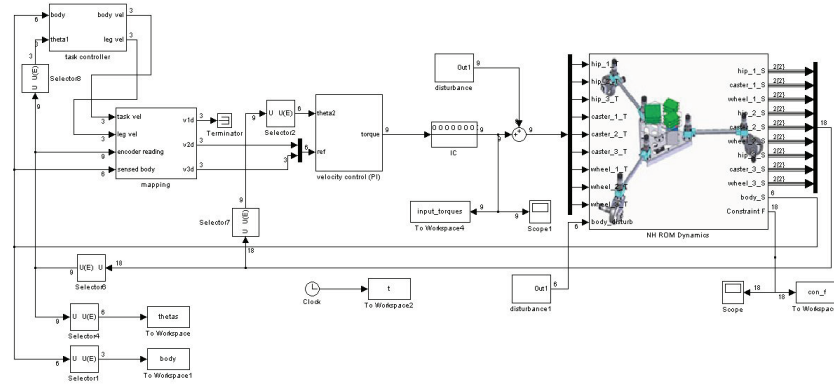


Fig. 5 Matlab RTW-based HIL Simulation

3.2 Results

Extensive simulation (based on SimMechanics model of the ROAMeR) and experimental testing was employed to evaluate performance of the developed control.

In the first case, the primary task is for the chassis to track a straight line in the x direction with an initial offset error of $0.1m$ in the y direction; the secondary task is for the legs to reconfigure from an initial fully extended configuration (hip angle $\theta_1 = 0^\circ$) to an almost fully compressed configuration (hip angle $\theta_1 = 90^\circ$) and then restore to initial configuration (hip angle $\theta_1 = 0^\circ$).

The simulation results in Fig. 6 shows satisfactory performance of the simultaneous locomotion and reconfiguration in the ideal case. The subsequent experimental results in Fig. 7 showcases the real world situation. Based on the noisy odometry feedback (blue dashed line), the controller manages to stay on path, however due to various factors like friction and backlash, the actual trajectory of the ROAMeR as captured by the motion tracking system (green dotted line) deviates a little bit from the reference. Snapshots of the line tracking video are shown in Fig. 8.

In the second case, the primary task is for the chassis to track a sine path in the x direction with an initial offset error of $0.05m$ in the y direction; the secondary task is for the legs to reconfigure from an initial fully extended configuration (hip angle $\theta_1 = 0^\circ$) to an almost fully compressed configuration (hip angle $\theta_1 = 90^\circ$).

Similar results are obtained for the sinusoidal tracking. Fig. 9 and Fig. 10 show-case the simulated and experimental performance of the simultaneous locomotion and reconfiguration. Snapshots of the sine tracking video are shown in Fig. 11.

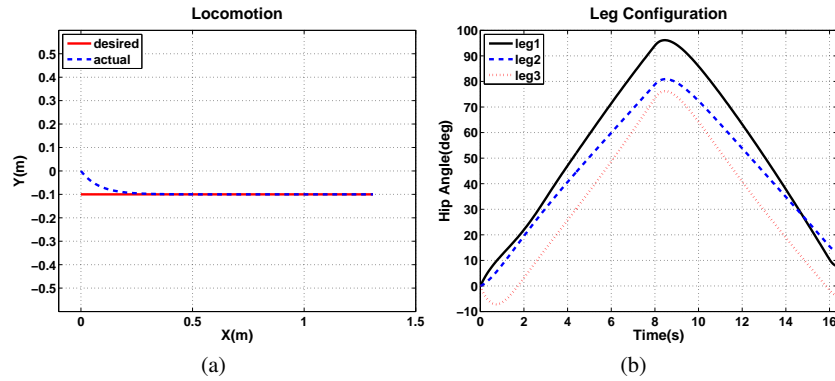


Fig. 6 Line Tracking Simulation (a) Cartesian Path-Following; (b) Hip-Joint Configuration

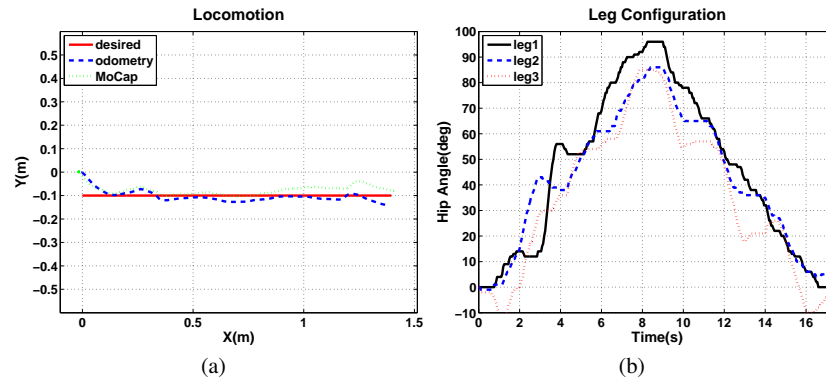


Fig. 7 Line Tracking Experiment (a) Cartesian Path-Following; (b) Hip-Joint Configuration

The results verify that the modeling and control methods developed in Sect. 2 are capable of controlling both the locomotion and reconfiguration behavior of the ROAMeR. Considering the low resolution (just the gear ratio) of the hall effect sensor encoders and low precision motors we used in the second prototype, the ROAMeR does a reasonably good job of tracking the desired trajectory. We will upgrade the hardware in our future design for better performance.

4 Main Experimental Insights

Articulated wheeled robots possess considerable advantages - by virtue of their reconfigurability and redundancy - which need to be unlocked by careful model-

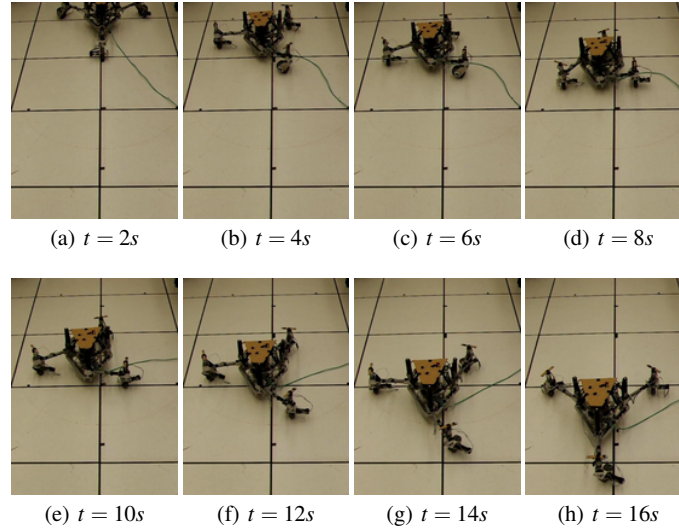


Fig. 8 Snapshots of Line Tracking

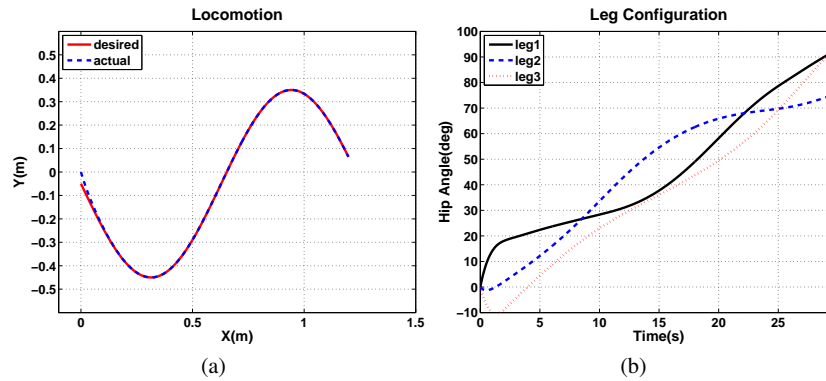


Fig. 9 Sine Tracking Simulation (a) Cartesian Path-Following; (b) Hip-Joint Configuration

ing, analysis and control. Hence we focused on developing a systematic twist- and wrench-based modeling framework, with an emphasis on symbolically modeling generic AWRs. This was illustrated on the Reconfigurable Omnidirectional Articulated Mobile Robot (ROAMeR) configuration. Two generations of physical prototypes were developed and several variants of simultaneous control of locomotion and reconfiguration were tested. Simulation-based testing with virtual prototypes were carried out prior to hardware-in-the-loop testing which allows us to verify the desired benefits of increased articulation and actuation i.e. better disturbance rejection with smaller motors. Enhancements including improved hardware design,

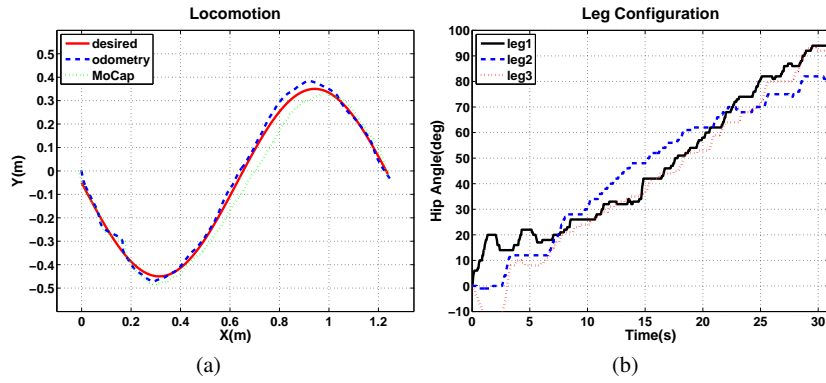


Fig. 10 Sine Tracking Experiment (a) Cartesian Path-Following; (b) Hip-Joint Configuration

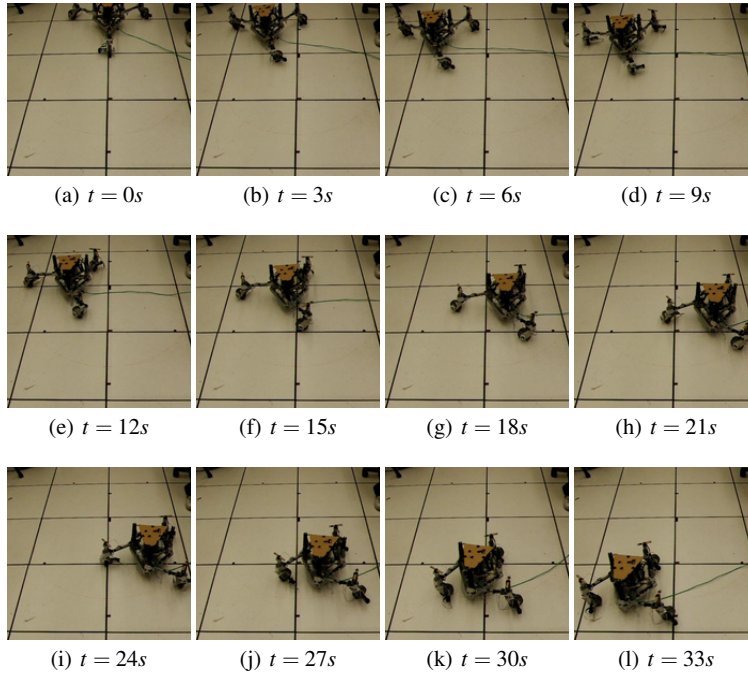


Fig. 11 Snapshots of Sine Tracking

inclusion of dynamic models and constraints, active reconfiguration planning and fully three-dimensional articulated-wheeled-robot designs are currently being pursued.

Acknowledgement

We gratefully acknowledge the support from the Research Foundation of State University of New York and National Science Foundation CNS-0751132.

References

1. Campion, G., Bastin, G., D'Andrea-Novell, B.: Structural properties and classification of kinematic and dynamic models of wheeled mobile robots. *IEEE Transactions on Robotics and Automation* **12**(1), 47–62 (1996)
2. Choi, B.J., Sreenivasan, S.V.: Partial contact force controllability in active wheeled vehicles. *Journal of Mechanical Design* **123**(2), 169–175 (2001)
3. Grand, C., Benamar, F., Plumet, F., Bidaud, P.: Stability and traction optimization of a reconfigurable wheel-legged robot. *International Journal of Robotics Research* **23**(10-11), 1041–1058 (2004)
4. Halme, A., Leppanen, I., Soumela, J., Ylonen, S., Kettunen, I.: Workpartner: interactive human-like service robot for outdoor applications. *International Journal of Robotics Research* **22**(7-8), 627–40 (2003)
5. Muir, P.F., Neuman, C.P.: Kinematic modeling of wheeled mobile robots. *Journal of Robotic Systems* **4**(2), 281–340 (1987)
6. Murray, R.M., Sastry, S.S., Zexiang, L.: *A Mathematical Introduction to Robotic Manipulation*. CRC Press, Inc. (1994)
7. Nakamura, Y.: *Advanced Robotics: Redundancy and Optimization*. Addison-Wesley Longman Publishing Co., Inc. (1990)
8. Siegwart, R., Lamon, P., Estier, T., Lauria, M., Piguat, R.: Innovative design for wheeled locomotion in rough terrain. *Robotics and Autonomous Systems* **40**, 151–162 (2002)
9. Sreenivasan, S.V., Waldron, K.J.: Displacement analysis of an actively articulated wheeled vehicle configuration with extensions to motion planning on uneven terrain. *Journal of Mechanical Design, Transactions of the ASME* **118**(2), 312–317 (1996)
10. Tarokh, M., McDermott, G.J.: Kinematics modeling and analyses of articulated rovers. *IEEE Transactions on Robotics* **21**(4), 539–553 (2005)
11. Wada, M., Asada, H.H.: Design and control of a variable footprint mechanism for holonomic omnidirectional vehicles and its application to wheelchairs. *IEEE Transactions on Robotics and Automation* **15**(6), 978–989 (1999)
12. Wilcox, B.H., Litwin, T.E., Biesiadecki, J.J., Matthews, J.B., Heverly, M.C., Morrison, J.C., Townsend, J.A., Ahmad, N.M., Sirota, A.R., Cooper, B.K.: Athlete: A cargo handling and manipulation robot for the moon. *Journal of Field Robotics* **24**(5), 421–434 (2007)
13. Yi, B.J., Kim, W.K.: The kinematics for redundantly actuated omnidirectional mobile robots. *Journal of Robotic Systems* **19**(6), 255–67 (2002)